

Antibiotic sensitization using biphenyl tetrazoles as potent inhibitors of *Bacteroides fragilis* metallo- β -lactamase

Jeffrey H Toney¹, Paula MD Fitzgerald¹, Nandini Grover-Sharma¹, Steven H Olson², Walter J May¹, Jon G Sundelof¹, Dana E Vanderwall¹, Kelly A Cleary¹, Stephan K Grant¹, Joseph K Wu¹, John W Kozarich¹, David L Pompliano¹ and Gail G Hammond¹

Background: High level resistance to carbapenem antibiotics in gram negative bacteria such as *Bacteroides fragilis* is caused, in part, by expression of a wide-spectrum metallo- β -lactamase that hydrolyzes the drug to an inactive form. Co-administration of metallo- β -lactamase inhibitors to resistant bacteria is expected to restore the antibacterial activity of carbapenems.

Results: Biphenyl tetrazoles (BPTs) are a structural class of potent competitive inhibitors of metallo- β -lactamase identified through screening and predicted using molecular modeling of the enzyme structure. The X-ray crystal structure of the enzyme bound to the BPT L-159,061 shows that the tetrazole moiety of the inhibitor interacts directly with one of the two zinc atoms in the active site, replacing a metal-bound water molecule. Inhibition of metallo- β -lactamase by BPTs *in vitro* correlates well with antibiotic sensitization of resistant *B. fragilis*.

Conclusions: BPT inhibitors can sensitize a resistant *B. fragilis* clinical isolate expressing metallo- β -lactamase to the antibiotics imipenem or penicillin G but not to rifampicin.

Introduction

Carbapenem antibiotics such as imipenem (Primaxin®) have proven to be useful for the treatment of a variety of gram negative and gram positive infections [1–3]. At the molecular level, carbapenems and other β -lactam antibiotics function by covalently modifying peptidoglycan biosynthetic enzymes responsible for catalyzing the final transpeptidation step of cell wall biosynthesis [4]. Inactivation of these ‘penicillin-binding proteins’ by carbapenem antibiotics leads to cell lysis [5]. Carbapenems are generally not hydrolyzed by class A serine-based β -lactamases [6] but are hydrolyzed rapidly by class B metallo- β -lactamases (Figure 1) [7] and are thus rendered ineffective.

Species of *Bacteroides*, including *Bacteroides fragilis*, are commonly found in clinical isolates from suppurative/surgical infections [8]. Treatment options for *B. fragilis* infections typically include β -lactam/carbapenem agents such as amoxicillin and imipenem. A potentially major medical concern is that bacteria may develop resistance to carbapenems in a similar manner to the widespread resistance currently observed for other β -lactam antibiotics. Antibiotic resistance mediated by class B β -lactamases is already emerging among *Bacteroides* species [9]. Simultaneous

Addresses: ¹Department of Biochemistry and ²Department of Basic Chemistry, Merck Research Laboratories, P. O. Box 2000, Rahway, NJ 07065-0900, USA.

Correspondence: Jeffrey H Toney and David L Pompliano
E-mail: jeff_toney@merck.com and david_pompliano@merck.com

Key words: antibiotic resistance, biphenyl tetrazoles, crystal structure, enzyme inhibitors, metallo- β -lactamase

Received: 10 November 1997
Revisions requested: 5 December 1997
Revisions received: 17 February 1998
Accepted: 23 February 1998

Published: 6 April 1998

Chemistry & Biology April 1998, 5:185–196
<http://biomednet.com/eleceref/1074552100500185>

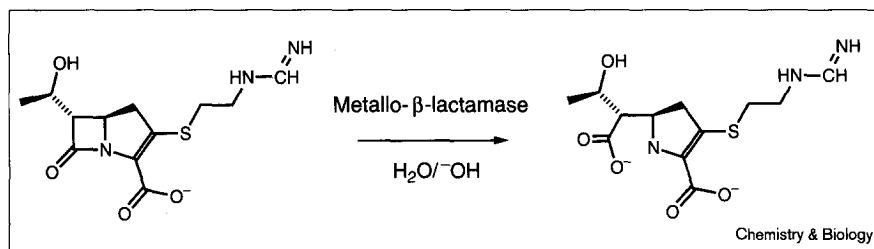
© Current Biology Ltd ISSN 1074-5521

resistance to metronidazole, co-amoxiclav (see below) and imipenem in a *B. fragilis* clinical isolate was reported recently [10] and was found to be due to an induced expression of a metallo- β -lactamase-like enzyme.

One strategy for overcoming bacterial resistance to antibiotics is to use combination therapy. Such a strategy has proven successful in combating resistance mediated by class A serine-based β -lactamases, for instance in treating bacterial infections normally resistant to agents such as amoxicillin. Co-amoxiclav (Augmentin™) is comprised of the β -lactam antibiotic amoxicillin and clavulanic acid, a ‘suicide’ inhibitor of the class A β -lactamases [11]. Augmentin™ is effective in treating β -lactamase-producing strains of staphylococci, *Hemophilus influenzae*, gonococci and *Escherichia coli*. Our interest has been to identify potent inhibitors of class B β -lactamases that may be useful in combination with carbapenem antibiotics against resistant bacterial strains.

Several genes encoding carbapenem and cephamycin resistance (*ccrA*) have been identified from independent isolates of *B. fragilis* [7] including the genes encoding the metallo- β -lactamases CcrA, CcrA3 and CcrA4. The three

Figure 1



The hydrolysis reaction of imipenem by metallo- β -lactamase.

encoded enzymes differ by four amino acids out of a total of 249 residues. The enzyme described here differs from CcrA by having threonine instead of alanine at residue 171 and asparagine instead of aspartate at residue 208. The crystal structure of the CcrA3 metallo- β -lactamase has been reported and reveals that the active site of the enzyme contains a binuclear zinc core [12]. The structure of metallo- β -lactamase from *Bacillus cereus* revealed a novel protein fold and one zinc atom in the active site [13], but more recent structural studies of the same enzyme reveal two zinc atoms in the active site (PDB entry 1BME). In the case of the CcrA sub-family of metallo- β -lactamases, the protein ligands of one of the zinc atoms, designated Zn 1, are three histidine residues whereas the ligands for Zn 2 are a histidine, an aspartic acid and a cysteine. In addition, the two zinc atoms are bridged by a water/hydroxide molecule, resulting in a tetrahedral geometry for Zn 1 and a trigonal bipyramidal geometry for Zn 2, which is axially coordinated to an additional water molecule. The catalytic mechanism of hydrolysis has been proposed to involve the bridging water/hydroxide between the two zinc atoms in the active site that can serve as the attacking nucleophile on the carbonyl carbon of the β -lactam (Figure 2a) [12]. In addition, both zinc atoms are thought to be required for full

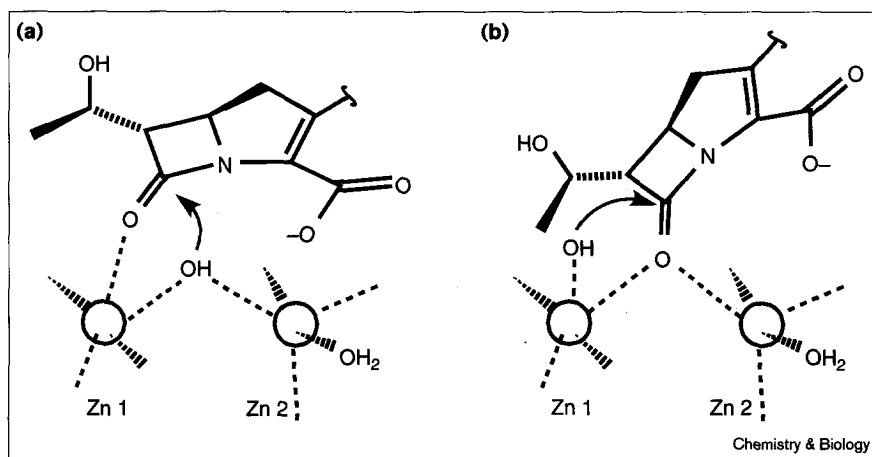
catalytic activity [14]. Further experiments will be necessary, however, to determine whether the attacking nucleophile is the bridging water/hydroxide or a water molecule bound at the axial position on Zn 1 (Figure 2b) after displacement of the bridging water/hydroxide by substrate.

Knowledge of the enzyme structure can provide insight into possible mechanisms of inhibition. As one may be able to predict and/or design molecules that can interact specifically with one or both of the zinc sites in the enzyme, compounds that selectively prevent substrate binding while not interfering with cellular zinc metabolism should be specific for metallo- β -lactamase. In contrast, compounds with high affinity for hydrated zinc (e.g., $[\text{Zn}(\text{H}_2\text{O})_6]^{2+}$ [15,16]) are expected to inhibit most Zn^{2+} -dependent enzymes for which the metal is accessible by a chelator and would not be of therapeutic interest.

The search for inhibitors of metallo- β -lactamase described in the present report employs screening techniques as well as use of the crystal structure of the enzyme for molecular docking of candidate inhibitors. These approaches have led to the identification of biphenyl tetrazoles (BPTs) as potent competitive inhibitors. This class of compounds

Figure 2

Two of the possible mechanisms for the hydrolysis of a carbapenem. In (a) the substrate binds with the β -lactam carbonyl oxygen interacting with Zn 1. The attacking nucleophile is the hydroxide ion bridging Zn 1 and Zn 2. The interaction between the carbonyl oxygen and Zn 1 draws electron density away from the carbonyl carbon making it more electrophilic, thereby facilitating nucleophilic addition of the hydroxide ion. Zn 1 and possibly Zn 2 would stabilize the negative charge on the oxygens of the subsequent tetrahedral intermediate. Alternatively, in (b) substrate binds with the β -lactam carbonyl oxygen bridging Zn 1 and Zn 2, displacing the formerly bridging hydroxide to an axial position on Zn 1. The axial bound hydroxide on Zn 1 is the attacking nucleophile, and the resultant intermediate would resemble that described in (a).



Chemistry & Biology

does not significantly affect mammalian dehydropeptidase I (DHP-I) [17,18], a metalloenzyme that is also capable of hydrolyzing imipenem [19] in addition to dehydropeptide substrates. Importantly, the inhibition of the purified recombinant metallo- β -lactamase by the BPT class of compounds is found to correlate well with the ability of the compounds to sensitize a *B. fragilis* imipenem-resistant clinical isolate to imipenem.

Results

Structure-activity relationships of biphenyl tetrazole metallo- β -lactamase inhibitors

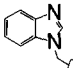
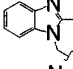
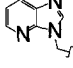
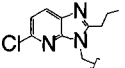
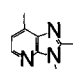
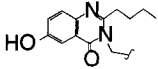
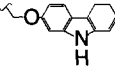
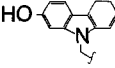
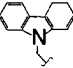
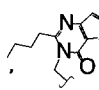
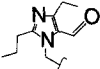
Screening of the Merck chemical collection using nitrocefin, a chromogenic cephalosporin, revealed a series of BPTs linked to various heterocyclic aromatic rings as inhibitors of metallo- β -lactamase. The unsubstituted BPT L-809,022 (R = H, Table 1) was found to be a poor inhibitor with an IC_{50} value of $860 \pm 60 \mu\text{M}$ and no detectable inhibition of DHP-I up to 1 mM. The ortho position of the tetrazole group relative to the biphenyl ring system was found to be important for enzyme inhibition because movement of the tetrazole group to the meta or para positions resulted in IC_{50} values of 10–20 mM. Substitution of carboxamide for the tetrazole group at the ortho position also led to a loss of activity ($IC_{50} > 20 \text{ mM}$). Similarly, movement of the carboxamide group to the meta or para positions led to a loss of activity with IC_{50} values of > 2.5 and $> 1.0 \text{ mM}$, respectively.

Inhibition of metallo- β -lactamase was increased significantly upon substitution at the 4'-position of the BPT. The parent compound L-158,507 (R = CH_3 , Table 1) had an IC_{50} of $160 \mu\text{M}$, a fivefold greater activity than L-809,022. Substitution at this benzylic position with various heterocyclic aromatic groups led to even further increases in activity. For example, addition of a benzimidazolyl fragment (L-808,509) resulted in a moderate increase in inhibition ($IC_{50} = 110 \mu\text{M}$), and incorporation of 2-methylbenzimidazole (L-809,559) led to a 40-fold increase in activity over the parent compound. The imidazo[4,5-*b*]pyridinyl group (L-809,558) was found to be slightly more inhibitory than the benzimidazolyl fragment. Elaboration of the imidazo[4,5-*b*]pyridinyl group with a propyl group at position 2 and a chlorine at position 5 (L-158,678) led to a potent compound having ~50-fold greater inhibition than the parent BPT. This inhibition could be increased further by substitution of a 7-methyl-2-(2-propyl)imidazopyridine (L-158,817). Interestingly, substitution of 2-butyl-6-hydroxylquinazolinone (L-159,061) led to a compound having ~100-fold greater inhibition than the parent BPT. As a whole, these BPTs with heterocyclic aromatic substitution showed little or no activity against DHP-I.

Metallo- β -lactamase inhibitors distinct from the benzimidazolyl or imidazopyridinyl class were also identified with little or no activity against DHP-I. An oxygen-linked

Table 1

Enzyme inhibition by BPTs.

Compound	R	IC_{50} (μM)	
		Metallo- β -lactamase	DHP-I
L-809,022	H	860 ± 60	>1000
L-158,507	CH_3	160 ± 20	>1000
L-808,509		110 ± 9	>500
L-809,559		4 ± 1	>250
L-809,558		42 ± 10	>250
L-158,678		3.5 ± 0.4	240 ± 12
L-158,817		1.8 ± 0.4	>100
L-159,061		1.9 ± 0.2	>100
L-809,339		42 ± 7	>100
L-809,370		6 ± 1	>100
L-161,189		0.30 ± 0.02	120 ± 10
L-159,906		0.4 ± 0.1	>100
L-707,581		7 ± 3	190 ± 8

2-hydroxycarbazolyl group (L-809,339) was found to be equipotent to the unsubstituted imidazopyridinyl compound L-809,558. Linking the 2-hydroxycarbazole via the nitrogen rather than the oxygen (L-809,370) significantly increased the inhibition, whereas removal of the 2-hydroxyl moiety led to a very potent inhibitor, L-161,189, that had ~500-fold greater activity than the parent BPT.

Potent inhibitors were also identified belonging to the BPT class containing 2-butyl-thieno[3,2-*d*]pyrimidin-4-one

(L-159,906) or 4-ethyl-2-propyl-imidazole-5-carboxaldehyde (L-707,581). Neither of these compounds inhibited DHP-I.

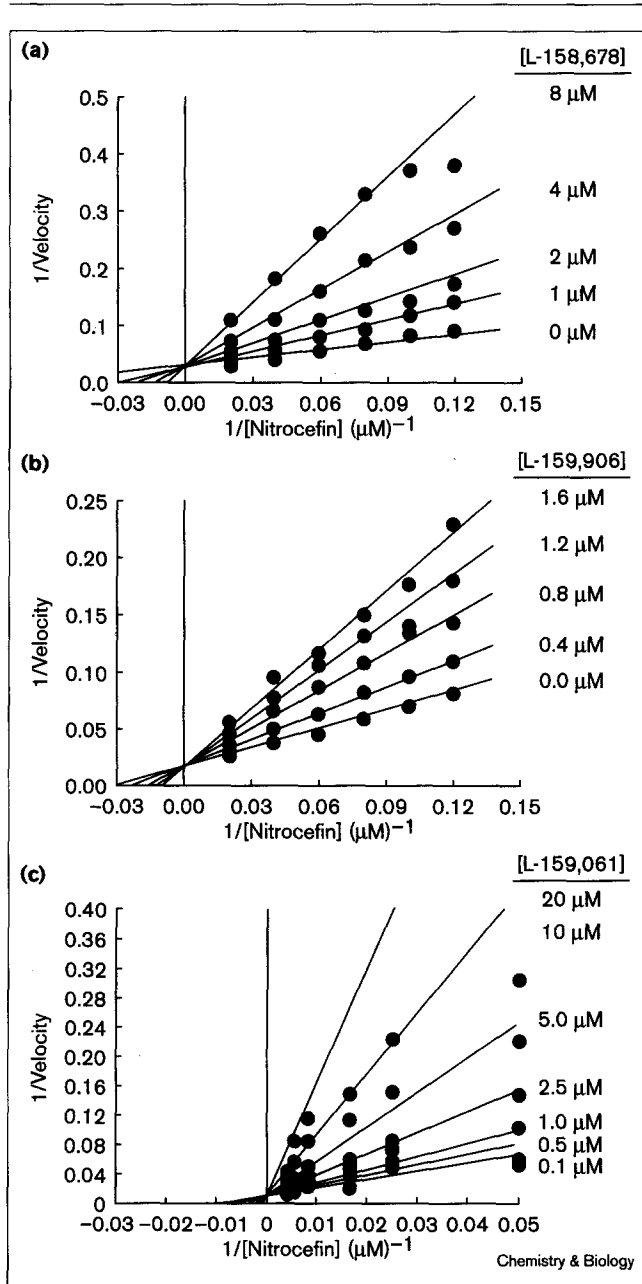
Three examples of the most potent inhibitors identified in the screen, L-158,678, L-159,906 and L-159,061 were studied in greater detail. These compounds were found to have simple competitive kinetics with the substrate nitrocefin, having K_i values of $1.5 \pm 0.1 \mu\text{M}$, $0.59 \pm 0.03 \mu\text{M}$ and $1.6 \pm 0.4 \mu\text{M}$ (Figure 3a–c), respectively. No time-dependent inhibition of metallo- β -lactamase by these compounds was observed under the same conditions employed to study enzyme inactivation (see below). To test for binding to metal ions, enzyme inhibition was measured after pre-incubation of the inhibitors with $100 \mu\text{M ZnCl}_2$. IC_{50} values of these compounds were unaffected by pre-incubation with ZnCl_2 within the uncertainty of the measurements.

In contrast, compounds such as bis(1*H*-tetrazol-5-yl)amine (L-295,819) that lack the biphenyl portion were found to be inactivators that inhibited the enzyme in a time-dependent fashion (Figure 4). The IC_{50} value for bis(1*H*-tetrazol-5-yl)amine was altered significantly by ZnCl_2 from $17 \mu\text{M}$ without pre-incubation to a value of $60 \mu\text{M}$ with pre-incubation, a result consistent with expected attributes of a metal chelator. Analysis of the kinetic data for bis(1*H*-tetrazol-5-yl)amine yielded a rate constant for inactivation of $k_{\text{inact}} = 0.52 \text{ min}^{-1}$ and $k_{\text{inact}}/K_i = 8900 \text{ M}^{-1}\text{s}^{-1}$. Interestingly, metal chelators such as 1,10-*o*-phenanthroline or tropolone were found to show time-dependent inhibition with similar rates of inactivation ($k_{\text{inact}} = 0.44$ and 0.62 min^{-1} , respectively). Thus, the rate-limiting step of inactivation could be dissociation of zinc from the enzyme active site.

Molecular modeling of candidate enzyme inhibitors

The determination of the X-ray crystal structure of the complex of metallo- β -lactamase bound to 4-morpholineethanesulfonic acid (MES) ($K_i \sim 23 \text{ mM}$) [20] allowed the opportunity to use a computational approach to search for inhibitors in parallel with the screening efforts used prior to the availability of a crystal structure of the enzyme bound to more potent inhibitors. A view of the enzyme active site complexed with MES is shown in Figure 5. The FLOG (flexible ligands oriented on a grid) [21–23] approach can scan a database of potential ligands by docking a three-dimensional structure into a grid representation of the active site and calculating an 'energy' or score for each docking. Grid-based energy evaluation is designed to circumvent the need to calculate all the pairwise interactions between the ligand and protein by representing the active site as an 'interaction energy field', sampled at uniformly spaced points in a three-dimensional grid [23–25]. At each point the potential energy within the active site is calculated and stored for each atom type used in the ligands. The score of a docked ligand is simply the sum of interaction energies for each ligand atom, based on the stored energies of the nearest grid points. In this study,

Figure 3

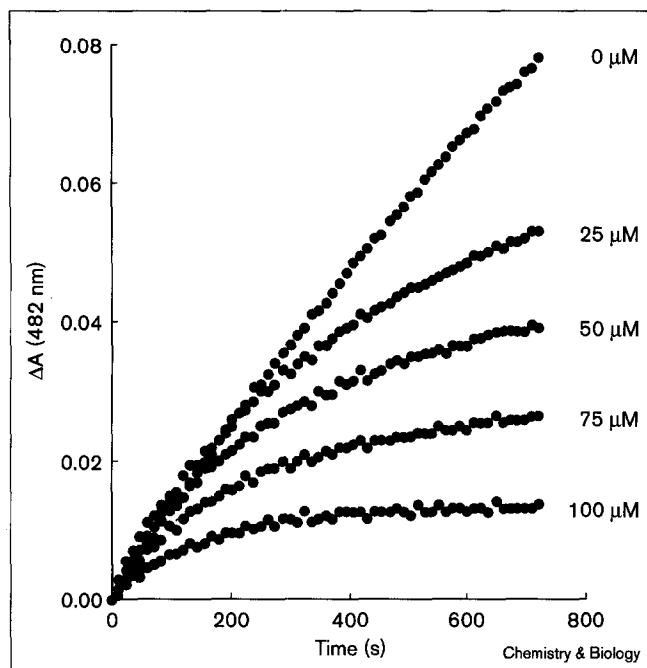


Biphenyl tetrazoles are competitive inhibitors of metallo- β -lactamase. Lineweaver-Burk plots consistent with competitive inhibition using the following BPTs: (a) L-158,678, (b) L-159,906 and (c) L-159,061. Data shown represent the average of two independent experiments.

the grids were calculated using residues within 6 \AA of the MES molecule found in the active site of the enzyme.

The observation of two zinc-bound water molecules/hydroxide groups suggested that several inhibitor-binding modes involving the metal centers might be possible. Consequently, several representations of the active site were used in grid and docking calculations and included

Figure 4

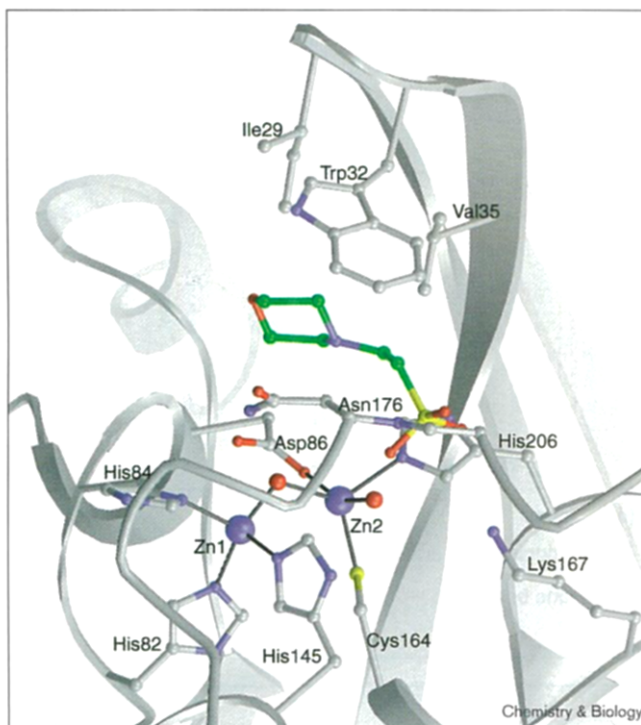


Time-dependent enzyme inhibition by bis(1*H*-tetrazol-5-yl)amine (L-295,819). Data shown are from a single representative experiment.

the combinations of waters and essential match centers shown in Figure 6. In each case $\sim 1.6 \times 10^6$ conformers were docked, and the best 100–500 scoring compounds from each calculation were chosen for measuring enzyme inhibition. Some compounds were predicted in more than one search, such that the following summaries describe only compounds not tested previously in the enzyme assay. The three searches yielded a total of 71 compounds that had IC_{50} values of $\leq 20 \mu\text{M}$, of which 56 were BPTs and 15 were compounds comprised of diverse classes referred to as non-BPTs. The compounds identified by the searches included the most potent BPTs containing heterocyclic aromatic groups identified concurrently in the screen for inhibitors. The active-site representation that included a bridging water/hydroxide and an essential match point at the position of the axial water bound to Zn 2 (Figure 6, representation iii) yielded 52 compounds with IC_{50} values of $\leq 20 \mu\text{M}$ out of a total of 427 tested samples and included 41 BPTs. Despite the finding that the non-BPTs identified in these calculations appeared to be potent metallo- β -lactamase inhibitors, most of these compounds were found either to bind to $ZnCl_2$ in the absence of enzyme or to act as enzyme inactivators (e.g., L-295,819). These inhibitors were therefore not chosen for subsequent biological studies.

Representation (iii) shown in Figure 6 was the most predictive, accounting for all but four of the inhibitors identified in these calculations. This suggested that the BPTs

Figure 5



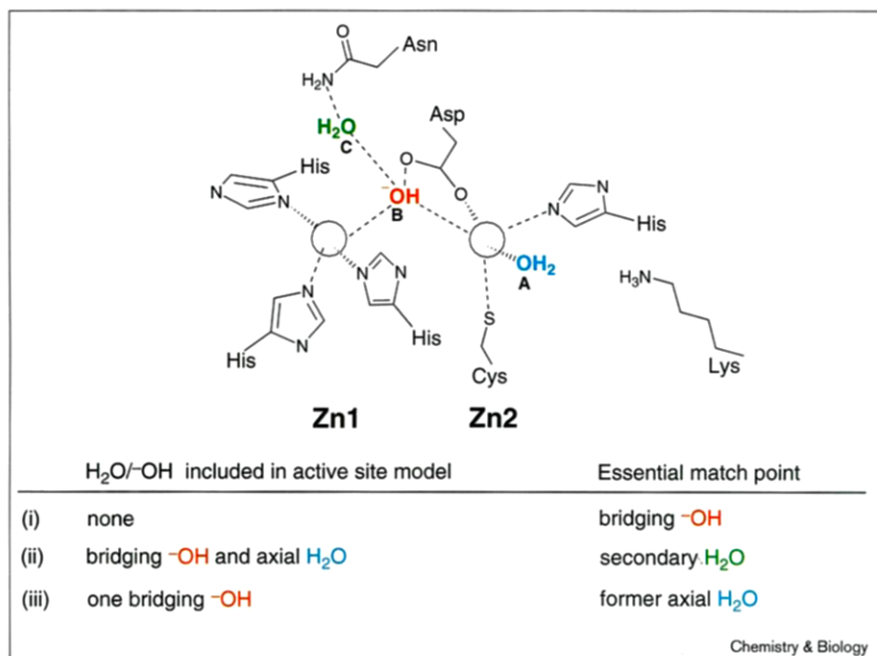
A view of the enzyme active site complexed with MES at 1.85 Å resolution. See [20] for structural details.

could bind with the tetrazole replacing the axial water as a ligand to Zn 2, placing the biphenyl group in contact with a hydrophobic region of a flexible β strand composed of residues 27–35 extending above the enzyme active site. Two orientations of BPTs in the active site were observed for this binding mode, shown in Figure 7. The orientation shown in Figure 7a was observed more frequently than that shown in Figure 7b, although each binding mode yielded similar scores.

Crystallography of metallo- β -lactamase bound to L-159,061: overall structure

As L-159,061 was found to be a potent competitive inhibitor, it was chosen for crystallographic studies to define the mode of BPT binding. An overview of the structure of the enzyme–inhibitor complex is shown in Figure 8. The enzyme consists of two domains, each of which contains a β sheet lined on one face by α helices. The two domains have similar topology [13], but the amino-terminal domain contains a feature not present in the carboxy-terminal domain: a β strand formed by residues 27–35. We refer to the β strand (residues 27–35) as the flap of the enzyme, as it exhibits marked plasticity in the structures of the metallo- β -lactamases determined to date [12,13,20] (PDB entry 1BME). The active site is situated at the interface between the two β sheets and the

Figure 6



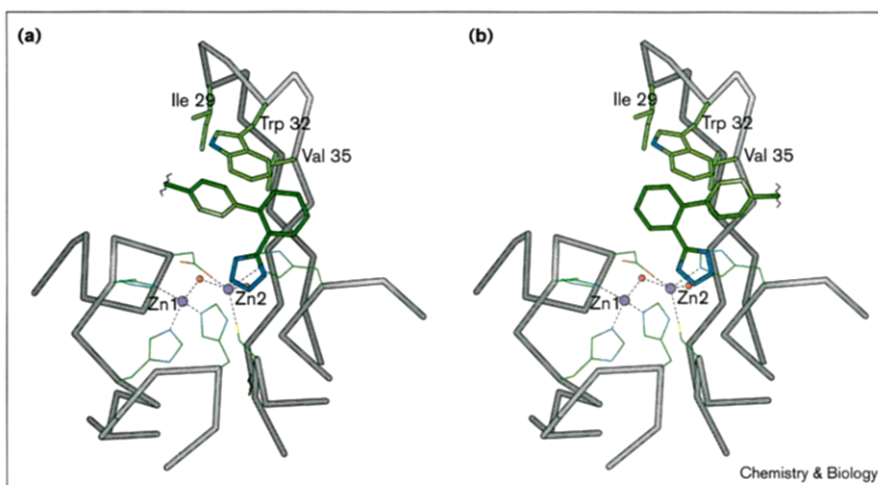
Representation of the enzyme active site employed for molecular modeling. Three different configurations (i–iii) of the active-site waters and essential match points were used in computational searches for candidate inhibitors. The left hand column describes which water or hydroxide molecules were included in each case. The right hand column describes the location of the essential match point in the search. The positions of the active-site waters observed in the X-ray crystal structure with MES are labeled and color coded as follows: A, axial water (blue) on Zn 2; B, hydroxide ion (red) bridging Zn 1 and Zn 2; C, secondary water (green) hydrogen bonded to the bridging hydroxide ion between the two zinc atoms.

BPT inhibitors bind in the cavity that is bounded by the active site and capped by the flap (Figure 8).

The organization of the binuclear zinc cluster in the inhibited complex is similar to that observed for the unliganded *B. fragilis* enzyme [12] and for the complex with MES [20]. A well-defined water molecule bridges the two zinc atoms in the unliganded enzyme structure and the MES complex, which are both refined to 1.85 Å, but there is no clear electron density at the position of the zinc-bridging

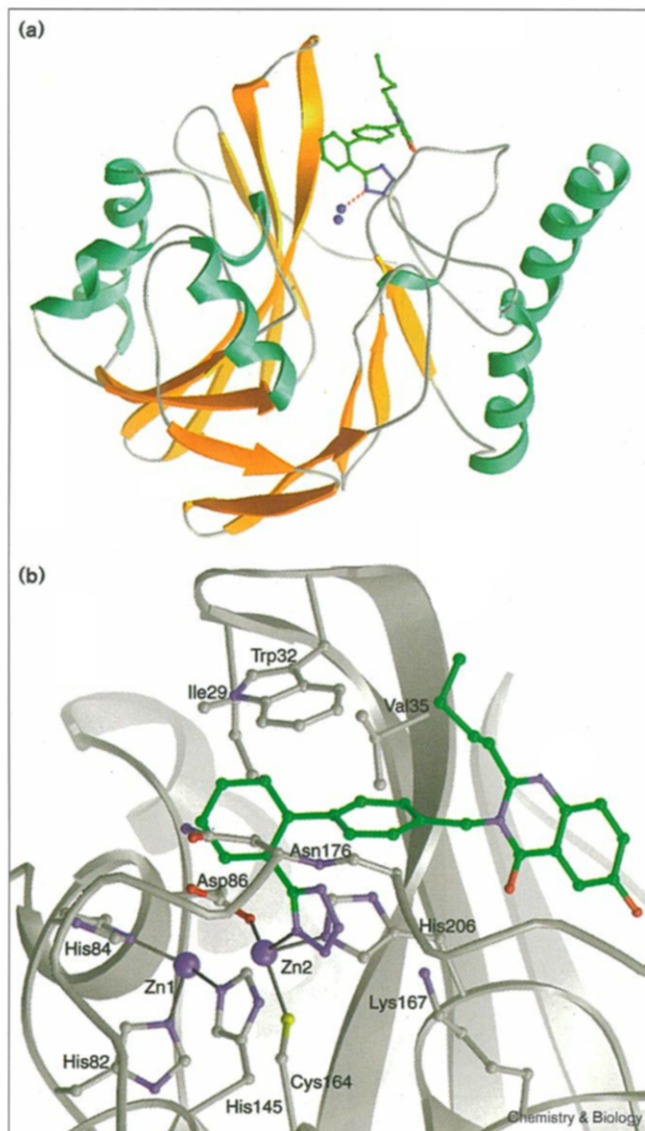
water molecule in the enzyme complex with L-159,061. At the resolution of the present crystal structure (2.55 Å, Tables 2 and 3), we cannot be certain of its presence or absence. Interestingly, a recent report of the crystal structure of the unliganded enzyme (2.0 Å resolution) indicates the absence of a water molecule bridging the two zinc atoms [26]. The coordination of Zn 2 is trigonal bipyramidal in the unliganded enzyme structure and the complex with MES in which the axial ligand was a water molecule. In the structure of the enzyme–L-159,061 complex, the

Figure 7



The two orientations for BPT binding predicted by molecular modeling using the FLOG algorithm. Both (a) and (b) involve the tetrazole (blue) replacing a water (red) on Zn 2 as a ligand, and an interaction between the biphenyl group and the hydrophobic sidechains of the flap. The position of the water (red) replaced by the tetrazole is shown for the purpose of illustration.

Figure 8



The X-ray crystal structure of L-159,061 bound in the active site of *B. fragilis* metallo- β -lactamase. (a) A ribbon diagram of the overall complex at 2.55 Å resolution. The two zinc atoms are shown as purple spheres, and the inhibitor is shown as a ball and stick model. The interaction between the inhibitor and Zn 2 is indicated by a red dashed line. (b) A view of the active site. The sidechain carbons and ribbon tracing of the α carbons are colored gray; nitrogens, oxygens and sulfur are purple, red and yellow, respectively. In the inhibitor, carbon, nitrogen and oxygen are green, purple and red, respectively. Interactions with the zinc are shown by black lines.

axial position is occupied by the N1 atom of the tetrazole moiety of the inhibitor. The N3 atom of the tetrazole ring interacts with a solvent atom that in turn interacts with the terminal nitrogen atom of the sidechain of LysA167, although the solvent atom is not well defined at the resolution of this structure. The N4 atom interacts with the amide nitrogen of AsnA176. The biphenyl portion of the

Table 2

Data collection statistics.

Resolution range (Å)	Number of reflections*	Completeness	Mean $Y/\sigma(Y)$ [†]	R_{merge} [‡]
∞ –4.63	2801	0.940	31.6	0.042
4.63–3.68	2462	0.875	13.1	0.070
3.68–3.21	2217	0.795	6.7	0.102
3.21–2.92	1960	0.716	4.1	0.125
2.92–2.71	1691	0.613	2.9	0.123
2.71–2.55	1468	0.538	2.4	0.125
∞ –2.55	12599	0.750	12.1	0.077

*The number of reflections with $I > \sigma(I)$. [†] $Y = \text{average of all observations of a given reflection}$. [‡] $R_{\text{merge}} = \frac{\sum_{\text{hkl}} \sum_i |I(\text{hkl},i) - \langle I(\text{hkl}) \rangle|}{\sum_{\text{hkl}} \sum_i I(\text{hkl},i)}$

inhibitor interacts with hydrophobic sidechains in the protein, principally provided by residues in the flap. The major enzyme–inhibitor interaction is observed between the second phenyl ring of the inhibitor and the sidechain of TrpA32, but there are also significant contacts with the sidechains of IleA29 and ValA35. The 6-hydroxyl position of L-159,061 interacts with O^{δ1} of AspA168 and more weakly with N^{δ2} of AsnA208. A second polar interaction involves the oxygen of the quinazolinone group and the water molecule that bridges the interaction between N3 of the tetrazole ring and the terminal nitrogen atom of the sidechain of LysA167. The remaining interactions with the protein are hydrophobic, involving the second phenyl group of the inhibitor, the butyl substituent of the quinazolinone, and the sidechains of TrpA32, ValA34 and ProA36. Further details of the structure of the enzyme–inhibitor complex of L-159,061 and related BPTs will be presented elsewhere (P.M.D.F., N.G.-S., S.H.O., J.K.W. and J.H.T., unpublished observations). Taken together, the crystallographic data are consistent with the binding mode shown in Figure 7b predicted by the FLOG algorithm.

Biological activity of biphenyl tetrazoles

To test the hypothesis of whether inhibition of metallo- β -lactamase expressed in imipenem-resistant *B. fragilis* would lead to sensitization of the cells to carbapenem or β -lactam antibiotics, a whole-cell agar diffusion assay was developed (see the Materials and methods section). Agar plates were prepared using an overnight culture of *B. fragilis* CLA 355 grown under anaerobic conditions and then diluted in the presence of a sub-inhibitory concentration of imipenem, penicillin G or rifampicin at $1/8 \times$ the minimal inhibitory concentration (MIC). Inhibitors or a dimethylsulfoxide (DMSO) vehicle control were then added to wells bored into the agar. Zones of inhibition were measured after incubation overnight. Addition of selected BPTs that had been identified as inhibitors of metallo- β -lactamase with an IC_{50} value of less than $\sim 40 \mu\text{M}$ led to significant zones of inhibition when imipenem or penicillin G

Table 3

Summary of refined model.

Root mean square deviation	σ	Value in model	Number of restraints		
			Total	>2 σ	>3 σ
From ideal bond distances					
Bond distances	0.020	0.018	3650	90	7
Angle distances	0.030	0.043	4981	508	166
Planar 1–4 distances	0.040	0.045	1325	64	29
From ideal planarity (\AA)	0.020	0.014	613	3	0
From ideal chirality (\AA^3)	0.150	0.209	562	56	21
From permitted contact distances (\AA)					
Single torsion contacts	0.500	0.261	1335	0	0
Multiple torsion contacts	0.500	0.333	1645	8	0
Possible H-bonds	0.500	0.301	249	1	0
From ideal torsion angles ($^\circ$)					
Planar groups (0 or 180)	3.0	2.4	460	7	0
Staggered groups (± 60 or 180)	15.0	24.7	590	98	47
Orthonormal groups (± 90)	20.0	25.6	52	3	2
Resolution range (\AA)			Number of reflections	R	
10.00–6.74			653	0.240	
6.74–5.43			841	0.218	
5.43–4.67			972	0.163	
4.67–4.15			1035	0.148	
4.15–3.78			1108	0.161	
3.78–3.49			1143	0.163	
3.49–3.26			1165	0.175	
3.26–3.07			1163	0.185	
3.07–2.91			1133	0.191	
2.91–2.78			1105	0.190	
2.78–2.66			1058	0.195	
2.66–2.55			952	0.188	
10.00–2.55			12328	0.181	

but not rifampicin were employed as potential antibiotics (Table 4 and Figure 9). Several of the BPTs had weak antibacterial activity against CLA 355. In addition to their own antibacterial activity, L-809,370 and L-161,189 were able to potentiate the effect of sub-lethal concentrations of imipenem against the *B. fragilis* strain.

Discussion

Some BPTs have been reported to be potent nonpeptide antagonists of the peptide angiotensin II (AII), an important biological target for the treatment of hypertensive disorders [27]. The mode of inhibition of these compounds with the AII receptor subtype AT_1 is proposed to involve a lysine–aromatic interaction via the tetrazole moiety of the BPT [28] and does not involve metal binding. In the present report, BPTs have been shown to be potent competitive inhibitors of metallo- β -lactamase using kinetic as

well as structural studies. Crystallographic studies of L-159,061 show that the tetrazole moiety displaces an axial water molecule bound to the Zn 2 atom within the active site of the enzyme, and that the biphenyl moiety forms favorable interactions with the hydrophobic residues of the flap extending above the active site. Such a mode of interaction is consistent with the observed kinetics of competitive inhibition of the enzyme in the presence of substrate.

The interaction between the tetrazole moiety of the BPT class and the active-site Zn 2 is not sufficient to account for the observed potent enzyme inhibition. The unsubstituted BPT L-809,022 is a weak inhibitor of metallo- β -lactamase. Thus, additional substituents are necessary to provide the strong binding interactions observed with compounds such as L-159,061 and L-161,189. Indeed, the determination of the crystal structure of the enzyme complexed with

Table 4

Effect of BPTs on susceptibility of *B. fragilis* CLA 355 to sub-MIC concentrations of antibiotics.

Compound	Zone size (mm)*				IC ₅₀ (μ M) [†]
	No addition	+ Imipenem 2 μ g/ml	+ Penicillin G 8 μ g/ml	+ Rifampicin 0.03 μ g/ml	
L-161,189	14	32	24	13	0.30 \pm 0.02
L-158,817	NZ	37	25	NZ	1.8 \pm 0.4
L-158,678	NZ	29	ND	NZ	3.5 \pm 0.4
L-809,559	NZ	29	17	NZ	4 \pm 1
L-809,370	12	34	24	12	6 \pm 1
L-809,558	NZ	14	NZ	NZ	42 \pm 10
L-809,339	10	11	NZ	NZ	42 \pm 7
L-809,022	NZ	NZ	NZ	NZ	860 \pm 60
DMSO Control	NZ	NZ	NZ	NZ	-

*Zones of inhibition produced by the BPTs against CLA 355 with and without addition of sub-MIC concentrations of antibiotic. [†]Measured using recombinant *B. fragilis* metallo- β -lactamase. NZ, no zone of inhibition detected; minimum detectable zone size is 7 mm. ND, not determined.

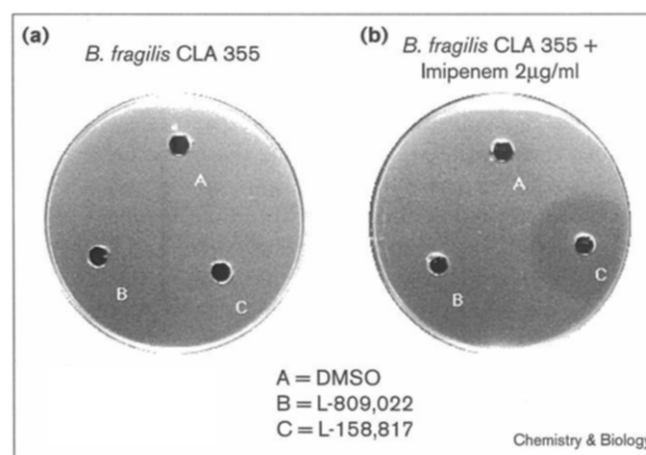
L-159,061 revealed that Trp32 present in the flexible β strand extending above the active site interacts with the second phenyl ring of the inhibitor as well as additional contacts between the enzyme and the quinazolinone group of the inhibitor. A mutation at residue 32 could conceivably lead to resistance to BPT inhibitors. It is noteworthy that a tryptophan at residue 32 or the equivalent position is conserved in metallo- β -lactamases found in the CcrA family and in IMP-1, a plasmid-mediated metallo- β -lactamase found in *Pseudomonas aeruginosa*, *Serratia marcescens* and in *Klebsiella pneumoniae* [7], but is deleted from metallo- β -lactamases found in *B. cereus*, *Aeromonas hydrophila* and *Stenotrophomonas maltophilia* [7]. In addition, the nature of the heterocyclic ring system (Table 1) has a dramatic effect on enzyme inhibition, consistent with the idea that specific interactions of this moiety with active-site residues are necessary for potent enzyme inhibition. In contrast, the interactions between the biphenyl portion of the inhibitor and the flap extending above the active site appear to be relatively nonspecific.

Knowledge of the structure of metallo- β -lactamase bound to MES allowed the use of molecular modeling techniques to complement the screening effort for enzyme inhibitors prior to the availability of a crystal structure of the enzyme bound to more potent inhibitors. An energy grid was generated to represent the enzyme active site for docking of conformers deposited in the Merck chemical database. The best 500 docking scores yielded 41 enzyme inhibitors belonging to the BPT class. An additional 15 inhibitors were identified in these searches that were distinct from the BPT class. The non-BPT inhibitors were found in general either to bind to ZnCl₂ or to act as enzyme inactivators and thus were not studied further. Interestingly, none of the searches identified any compounds structurally related to a

known substrate or the MES molecule in the original crystal structure [20]. The success of this docking technique demonstrates that prediction of enzyme inhibitors using algorithms such as FLOG can rapidly enhance the testing of available compounds by focusing on chemical classes that interact with the active site in a favorable manner.

Inhibitors of metallo- β -lactamases belonging to chemical classes unrelated to BPTs have been reported. Mercaptoacetic acid thiol esters are irreversible inhibitors of metallo- β -lactamases from *B. cereus*, *Stenotrophomonas maltophilia*

Figure 9



Reversal of antibiotic resistance in a clinical isolate of *B. fragilis* by a BPT in synergy with imipenem. (a) Neither L-158,817 or L-809,022 alone produces zones of inhibition against CLA 355. (b) In contrast, L-158,817 synergizes with imipenem, as shown by a zone of inhibition, whereas L-809,022, a weak metallo- β -lactamase inhibitor, does not synergize with imipenem. DMSO is included as a solvent control.

and *Aeromonas hydrophila* but not from *B. fragilis* [29]. Thiol esters have been shown to inhibit the *B. cereus* enzyme via hydrolytic release of mercaptoacetic acid which subsequently covalently modifies a cysteine residue at the active site. That the *B. fragilis* enzyme is not significantly inhibited by the thiol esters suggests that the analogous active-site cysteine in this protein is less accessible to such inhibitors. Trifluoromethyl alcohol and ketone derivatives of L- or D-alanine have been reported to be competitive inhibitors of a metallo- β -lactamase from *Xanthomonas maltophilia* but not from *B. cereus* or *Pseudomonas aeruginosa* [30]. These compounds are proposed to bind to one of the Zn atoms in the active site as observed with the metalloenzyme carboxypeptidase A [31]. To date, none of the classes of inhibitors described above including the BPTs (data not shown) show a broad spectrum of activity against all known metallo- β -lactamases, emphasizing the structural heterogeneity of these enzymes.

Studies using the metalloenzyme DHP-I reveal that the BPTs do not interact significantly with DHP-I. Both the absence of DHP-I inhibition and the lack of effect of $ZnCl_2$ on the inhibition constants of metallo- β -lactamase argue against this class of compounds acting as nonspecific metal chelators. Taken together, these results indicate that the accessibility of compounds such as BPTs to the active site of metallo- β -lactamase and that of DHP-I are very different even though both enzymes are capable of hydrolyzing the same substrates.

The biological activity of several representative BPTs against imipenem-resistant *B. fragilis* in synergy with imipenem or penicillin G highlights the potential use of such agents in the battle against resistant bacteria. Whole-cell activity was found to correlate well with inhibition data of purified metallo- β -lactamase (Table 4). One possible explanation for the observed biological activity is that the BPTs increase cell permeability to the antibiotic, but the BPTs did not sensitize imipenem-resistant *B. fragilis* to rifampicin, an antibiotic that inhibits the initiation of RNA synthesis but not cell-wall biosynthesis, arguing against this possibility. Several of the BPTs were found to have small zones of inhibition in the absence of added antibiotic and this activity could be a result of the inhibition of cellular mechanisms other than inhibition of metallo- β -lactamases. In addition, two of the BPTs had small zones of inhibition in the presence of rifampicin but the size of these inhibition zones was similar to those (within experimental error) observed using the BPT in the absence of added antibiotic.

Significance

Drug resistance in bacteria is becoming an alarming problem worldwide and has been attributed, in part, to overuse of antibiotics [32] and to the expression of hydrolytic enzymes in bacteria that render antibiotics ineffective. One approach to the problem is to inhibit

chemically a specific protein target that has been shown to play a major role in drug resistance such as the class B metallo- β -lactamases. Such inhibitors would not necessarily be expected to act as antibiotics in their own right but have the potential to increase the effectiveness of antibiotics already employed. Recently, the phenotypic conversion of a drug-resistant bacterium to drug sensitivity has been accomplished genetically by a novel approach employing small oligoribonucleotides that cleave specifically the mRNAs encoding chloramphenicol acetyl transferase or a serine-based β -lactamase [33]. The pharmacological and computational approach discussed in the present report describes the phenotypic conversion of a resistant clinical strain through the use of metallo- β -lactamase inhibitors as a first step towards combating drug resistance in bacteria.

Materials and methods

Purified recombinant metallo- β -lactamase was prepared as described previously [34] and differs from CcrA (Genbank accession number M63556) by having threonine instead of alanine at residue 171 and asparagine instead of aspartate at residue 208.

Metallo- β -lactamase assays

Metallo- β -lactamase activity was assessed using the chromogenic substrate nitrocefin [35]. Enzyme preparations were diluted in 50 mM 4-morpholinepropanesulfonic acid (MOPS), pH 7.0 in a 96 well microtiter plate. A tenfold concentrated stock of nitrocefin was prepared in 50% DMSO. Experiments employing a fixed substrate concentration used nitrocefin at 20 μ M ($\sim K_m$) and enzyme at ~ 5 nM. After incubating enzyme at 37°C for 15 m in the presence of inhibitor, reactions were initiated by addition of nitrocefin with a final volume of 100 μ l. Nitrocefin hydrolysis was monitored at 482 nm using a Molecular Devices SpectraMax 250 microtiter plate reader. Reaction rates were linear from 3–5 min at 37°C. Stock solutions of inhibitors were typically prepared in 100% DMSO at 2–200 mM concentration. Enzyme activity was not significantly affected by addition of up to 20% DMSO (v/v). Initial velocities (v_i) were measured and converted to % inhibition (%INH) using $\%INH = 100 - (v_i(\text{with inhibitor})/v_i(\text{without inhibitor})) \times 100$. IC_{50} values were calculated as the concentration of inhibitor at which 50% of the enzyme activity is inhibited using an in-house software package (Jim McGurk, MRL). Standard deviations reported for IC_{50} values represent between three and six independent determinations. Reported values for K_i were determined using a model for competitive inhibition:

$$y = V_{max} \cdot x_1 / (x_1 + K_m \cdot (1 + x_2/K_i)) \quad (1)$$

where y = initial velocity of hydrolysis, x_1 = concentration of nitrocefin, x_2 = concentration of inhibitor.

Time-dependent inhibition was evaluated by fitting nonlinear progress curves to the first-order expression: $y = a_0 (1 - e^{-kt})$ where y is the concentration of hydrolyzed product accumulated at each time point, a_0 is the total amount of product formed, k is the observed first-order rate constant, k_{obs} , and t is assay time. Kinetic parameters for inactivation were determined using replots of half life $t_{1/2}$ as a function of the reciprocal of inhibitor concentration [36,37]. SigmaPlot software (version 4.14, Jandel Scientific) and MacNlin (in house software for nonlinear regression) were employed for fitting of data and error analysis.

Renal dehydropeptidase I assays

Reactions were carried out in 50 mM MOPS buffer, pH 7.1 using 10 μ l purified porcine DHP-1 (5 μ g/ml) at 37°C. After equilibration for 5 min, substrate glycyldehydrophenylalanine ($K_m \sim 0.6$ mM) was added to yield a final concentration of 50 μ M. Rates of substrate hydrolysis were

monitored for 15 min by measuring the decrease in absorbance at 275 nm. Rates were fit to the equation:

$$y = (a)(e^{-kt}) + c \quad (2)$$

where $a = A_{275\text{nm}}$ of the substrate in the presence of inhibitor at time zero, $c = \text{final } A_{275\text{nm}}$ and k is the rate constant. Enzyme was isolated as described [38] with the modification that the renal cortex was homogenized using 20% butanol in 20 mM MOPS buffer, pH 7.1.

Chemical synthesis of BPTs

The BPT compounds described in this study were prepared using well-established procedures [39]. Bis(1*H*-tetrazol-5-yl)amine (L-295,819) was obtained from Chembridge (Glenview, IL, USA). All other chemicals were of reagent grade.

Crystallization and data collection

A complex between L-159,061 and the metallo- β -lactamase from *B. fragilis* was crystallized in space group P2₁2₁2₁ by vapor diffusion equilibration against a solution containing 100 mM sodium cacodylate buffer, pH 6.6, 100 mM NaCl, 10 mM sodium acetate and 28% (w/v) polyethylene glycol (PEG 4000). The cell constants were $a = 71.36 \text{ \AA}$, $b = 170.23 \text{ \AA}$ and $c = 40.66 \text{ \AA}$. A summary of data processing statistics is presented in Table 2. The structure was solved by the molecular replacement method [40], using the model of the enzyme complexed to MES as the probe structure [20]. A model for the complex was refined using the program Prolog [41] against data extending from 10.0 to 2.55 \AA in resolution. The R-factor for the final model was 0.181 and deviations from ideal bond distances were 0.018 \AA . R_{free} was not monitored during refinement, although a cross-validation value of 0.306 was calculated for the final model. The quality and statistics of the refined model are summarized in Table 3. The coordinates have been deposited with the Protein Data Bank (entry code 1A8T). Full details of the crystallographic analysis will be published elsewhere. Figures 5 and 8 were created using the program Ribbons [42].

Molecular modeling

Using the X-ray crystal structure of *B. fragilis* determined recently with MES bound in the active site [20] the FLOG system for database searching and docking was used to identify enzyme inhibitors as described [21–23]. Following the addition of polar hydrogens and assignment of hydrogen bonds and appropriate tautomeric states of imidazoles, the grids used to represent the active site were calculated with 0.3 \AA spacing, and included the entire residue of any atom within 6 \AA of the MES molecule. In the formalism of the grid calculation, the zinc atoms are treated as a hydrogen-bond donor, without the angular term [21]. Consequently, favorable metal ligands will be hydrogen-bond acceptors. Neither formal charge nor metal-ligand bonds are considered in this type of potential energy function.

The grids and subsequent dockings were calculated including two, one or none of the waters observed in the X-ray crystal structure directly bound to a zinc ion. Neither the MES nor any other waters were included in the calculations. Match centers for docking ligands were generated at favorable interaction sites in the grid. The databases of three-dimensional structures or flexibases [23] contained typically between 5 and 25 conformations of each candidate inhibitor, using heavy atoms represented by 5 atom types (hydrogen bond donors, hydrogen bond acceptors, polar (both donor and acceptor), hydrophobic and other) as previously described.

Biological assays

The imipenem-resistant *Bacteroides fragilis* clinical isolate, CLA 355, from which metallo- β -lactamase was cloned [34] was used in an agar diffusion model to evaluate enzyme inhibitors for their ability to increase the susceptibility of resistant bacteria to antibiotics. CLA 355 was grown overnight at 37°C under anaerobic conditions (AnaeroGen system from Oxoid) in Schaedler's broth supplemented with vitamin K (Becton Dickinson). Agar plates (20 ml in 100 mm petri dishes) were prepared using Wilkins-Chalgren agar (Difco) inoculated with a 1:50 dilution of the

overnight *B. fragilis* culture containing imipenem at 2 $\mu\text{g/ml}$ or penicillin G at 8 $\mu\text{g/ml}$ (1/8 \times MIC). An agar plate containing no antibiotic served as a control for assessing the antibacterial activity of inhibitors alone. A rifampicin-containing plate (0.03 $\mu\text{g/ml}$) served as a non- β -lactam control. A 2 mM solution of each inhibitor (20 μl) was placed into 7 mm wells in the agar and zones of inhibition were measured following overnight incubation at 37°C in an anaerobic environment.

Acknowledgements

We wish to thank Vincent Pecoraro (University of Michigan, Ann Arbor) and Milton Hammond for critical comments on this manuscript, Lynn Silver for helpful suggestions for the whole-cell experiments and Barbara Leiting for advice regarding protein expression and purification. We would also like to thank members of the Molecular Systems Department (MRL) especially Robert P. Sheridan and Michael D. Miller. K.A.C. was supported by the Merck Research Laboratories Summer Intern Program.

References

- Jacobs, R.F. (1986). Imipenem-cilastatin: the first thienamycin antibiotic. *Pediatr. Infect. Dis. J.* **5**, 444-448.
- Clissold, S.P., Todd, P.A. & Campoli-Richards, D.M. (1987). Imipenem/cilastatin: a review of its antibacterial activity, pharmacokinetic properties and therapeutic efficacy. *Drugs* **33**, 183-241.
- Buckley, M. M., Brogden, R.N., Barradell, L.B. & Goa, K.L. (1992). Imipenem/cilastatin: a reappraisal of its antibacterial activity, pharmacokinetic properties and therapeutic efficacy. *Drugs* **44**, 408-444.
- de Lancastre, H., de Jonge, B.L.M., Matthews, P.R. & Tomasz, A. (1994). Molecular aspects of methicillin resistance in *Staphylococcus aureus*. *J. Antimicrob. Chemother.* **33**, 7-24.
- Mulligan, M.E., *et al.*, & Yu, V.L. (1993). Methicillin-resistant *Staphylococcus aureus*: A consensus review of the microbiology, pathogenesis, and epidemiology with implications for prevention and management. *Am. J. Med.* **94**, 313-328.
- Knox, J.R., Moews, P.C. & Frère, J.-M. (1996). Molecular evolution of bacterial β -lactam resistance. *Chem. Biol.* **3**, 937-947.
- Rasmussen, B.A. & Bush, K. (1997). Carbapenem-hydrolyzing β -lactamases. *Antimicrob. Agents Chemother.* **41**, 223-232.
- Rasmussen, B.A., Bush, K. & Tally, F.P. (1993). Antimicrobial resistance in *Bacteroides*. *Clin. Infect. Dis.* **16**, S390-S400.
- Hedberg, M. & Nord, C.E. (1996). Beta-lactam resistance in anaerobic bacteria: a review. *J. Chemother.* **8**, 3-16.
- Turner, P., Edwards, R., Weston, V., Grazis, A., Ispahani, P. & Greenwood, D. (1995). Simultaneous resistance to metronidazole, co-amoxiclav, and imipenem in a clinical isolate of *Bacteroides fragilis*. *Lancet* **345**, 1275-1277.
- Mandell, G.L. & Sande, M.A. (1985). Antimicrobial Agents. In *Goodman and Gilman's The Pharmacological Basis of Therapeutics*. (Goodman Gilman, A., Goodman, L.S., Rall, T.W. & Murad, F., eds), p.1145, Macmillan Publishing Co., New York.
- Concha, N.O., Rasmussen, B.A., Bush, K. & Herzberg, O. (1996). Crystal structure of wide-spectrum binuclear zinc β -lactamase from *Bacteroides fragilis*. *Structure* **4**, 823-836.
- Carfi, A., *et al.*, & Dideberg, O. (1995). The 3-D structure of a zinc metallo- β -lactamase from *Bacillus cereus* reveals a new type of protein fold. *EMBO J.* **14**, 4914-4921.
- Crowder, M.W., Wang, Z., Franklin, S.L., Zovinka, E.P. & Benkovic, S.J. (1996). Characterization of the metal-binding sites of the β -lactamase from *Bacteroides fragilis*. *Biochemistry* **35**, 12126-12132.
- Lippard, S.J. & Berg, J.M. (1994). *Principles of Bioinorganic Chemistry*, pp. 25 and 271, University Science Books, Mill Valley, CA.
- Hartmann, M., Clark, T. & van Eldik, R. (1997). Hydration and water exchange of Zinc (II) ions. Application of density functional theory. *J. Am. Chem. Soc.* **119**, 7843-7850.
- Harper, C., Rene, A. & Campbell, B.J. (1971). Renal dipeptidase: localization and inhibition. *Biochim. Biophys. Acta* **242**, 446-458.
- Welch, C.L. & Campbell, B.J. (1980). Uptake of glycine from L-alanyl-glycine into renal brush border vesicles. *J. Membr. Biol.* **54**, 39-50.
- Mitsuhashi, S., Fuse, A., Mikami, H., Saino, Y. & Inoue, M. (1988). Purification and characterization of human renal dehydropeptidase I. *Antimicrob. Agents Chemother.* **32**, 587-588.
- Fitzgerald, P.M.D., Wu, J.K. & Toney, J.H. (1998). Unanticipated inhibition of the metallo- β -lactamase from *Bacteroides fragilis* by 4-morpholineethanesulfonic acid (MES): a crystallographic study at 1.85 \AA resolution. *Biochemistry*, in press.

21. Miller, M.D., Kearsley, S.K., Underwood, D.J. & Sheridan, R.P. (1994). FLOG: A system to select 'quasi-flexible' ligands complementary to a receptor of known three-dimensional structure. *J. Comput. Aided Mol. Des.* **8**, 153-174.
22. Miller, M.D., Sheridan, R.P., Kearsley, S.K. & Underwood, D.J. (1994). Advances in automated docking applied to human immunodeficiency virus type protease. *Methods Enzymol.* **241**, 354-370.
23. Kearsley, S.K., Underwood, D.J., Sheridan, R.P. & Miller, M.D. (1994). Flexibases: a way to enhance the use of molecular docking methods. *J. Comput.-Aided Mol. Design* **8**, 565-582.
24. Meng, E.C., Shoichet, B.K. & Kuntz, I.D. (1992). Automated docking with grid-based energy evaluation. *J. Comput. Chem.* **13**, 505-524.
25. Lawrence, M. C. & Davis, P. C. (1992). CLIX: A search algorithm for finding novel ligands capable of binding proteins of known three-dimensional structure. *Proteins: Struct. Funct. Genet.* **12**, 13-41.
26. Carfi, A., Duée, E., Paul-Soto, R., Galleni, M., Frère, J.-M. & Dideberg, O. (1998). X-ray structure of the Zn^{II} β -lactamase from *Bacteroides fragilis* in an orthorhombic crystal form. *Acta Crystallogr. D* **54**, 47-57.
27. Ashton, W.T., et al., & Siegl, P.K.S. (1993). Nonpeptide angiotensin II antagonists derived from 1H-pyrazole-5-carboxylates and 4-aryl-1H-imidazole-5-carboxylates. *J. Med. Chem.* **36**, 3595-3605.
28. Noda, K., et al., & Karnik, S. (1995). Tetrazole and carboxylate groups of angiotensin receptor antagonists bind to the same subsite by different mechanisms. *J. Biol. Chem.* **270**, 2284-2289.
29. Payne, D.J., et al., & Marchand-Brynaert, J. (1997). Inhibition of metallo- β -lactamases by a series of mercaptoacetic acid thiol ester derivatives. *Antimicrob. Agents Chemother.* **41**, 135-140.
30. Walter, M.W., et al., & Schofield, C.J. (1996). Trifluoromethyl alcohol and ketone inhibitors of metallo- β -lactamases. *Bioorg. Med. Chem. Lett.* **6**, 2455-2458.
31. Christianson, D.W. & Lipscomb, W.N. (1986). The complex between carboxypeptidase A and a possible transition state analogue: mechanistic inferences from high resolution X-ray structures of enzyme-inhibitor complexes. *J. Am. Chem. Soc.* **108**, 4998-5003.
32. Williams, R.J. & Heymann, D.L. (1998). Containment of antibiotic resistance. *Science* **279**, 1153-1154.
33. Guerrier-Takada, C., Salavati, R. & Altman, S. (1997). Phenotypic conversion of drug-resistant bacteria to drug sensitivity. *Proc. Natl Acad. Sci. USA* **94**, 8468-8472.
34. Toney, J.H., Wu, J.K., Overbye, K.M., Thompson, C.M. & Pompliano, D.L. (1997). High-yield expression, purification, and characterization of active, soluble *Bacteroides fragilis* metallo- β -lactamase, CcrA. *Protein Expr. Purif.* **9**, 355-362.
35. O'Callaghan, C.H., Morris, A., Kirby, S.M. & Shingler, A.H. (1972). Novel method for detection of β -lactamases using a chromogenic cephalosporin substrate. *Antimicrob. Agents Chemother.* **1**, 283-288.
36. Kitz, R. & Wilson, I.B. (1962). Esters of methanesulfonic acid as irreversible inhibitors of acetylcholinesterase. *J. Biol. Chem.* **237**, 3245-3249.
37. Silverman, R.B. (1988). *Mechanism-Based Enzyme Inhibition: Chemistry and Enzymology*. (Volume 1), pp 12-23, CRC Press, Boca Raton, FL.
38. Kropp, H., Sundelof, J.G., Hadju, R. & Kahan, F.M. (1982). Metabolism of thienamycin and related carbapenem antibiotics by the renal dipeptidase, dehydropeptidase I. *Antimicrob. Agents Chemother.* **22**, 62-70.
39. Mantlo, N.B., et al., & Greenlee, W.J. (1991). Potent, orally active imidazo[4,5-b]pyridine-based angiotensin II receptor antagonists. *J. Med. Chem.* **34**, 2919-2922.
40. Fitzgerald, P.M.D. (1988). MERLOT, an integrated package of computer programs for the determination of crystal structures by molecular replacement. *J. Appl. Cryst.* **21**, 273-278.
41. Hendrickson, W.A. (1985). Stereochemically restrained refinement of macromolecular structures. *Methods Enzymol.* **115**, 252-270.
42. Carson, M. (1997). Ribbons. *Methods Enzymol.* **277**, 493-505.